University of Massachusetts Amherst
ScholarWorks@UMass Amherst

Physics Department Faculty Publication Series | Physics

2008

Unusual States of Vortex Matter in Mixtures of Bose-Einstein Condensates on Rotating Optical Lattices

E. K. Dahl

E. Babaev
University of Massachusetts - Amherst, babaev1@physics.umass.edu

A. Sudbø

Unusual states of vortex matter in mixtures of Bose–Einstein Condensates on rotating optical lattices

E. K. Dahl[1], E. Babaev[2,3] and A. Sudbø[1]
[1]Department of Physics, Norwegian University of Science and Technology, N-7491 Trondheim, Norway
[2]Physics Department, University of Massachusetts, Amherst MA 01003, USA
[3]Department of Theoretical Physics, The Royal Institute of Technology 10691 Stockholm, Sweden
(Dated: November 15, 2008)

In a single-component superfluid under rotation a broken symmetry in the order parameter space results in a broken translational symmetry in real space: a vortex lattice. If translational symmetry is restored, the phase of the order parameter disorders and thus the broken symmetry in the order parameter space is also restored. We show that for Bose-Condensate mixtures in optical lattices with negative dissipationless drag, a new situation arises. This state is a modulated vortex liquid which breaks translational symmetry in the direction transverse to the rotation vector.

An important property of a superfluid is its specific rotational response. Namely it comes into rotation by means of the formation of a vortex lattice. Under the influence of other factors such as temperature, multiplicity of superfluid components, inhomogeneities etc., different “aggregate” states of vortex matter may form, such as vortex liquids, glasses, etc [1]. The variety of states is even richer in multicomponent systems [2]. The transitions between the various “aggregate” states of vortex matter are related to various ordering processess of particles in condensed matter systems. For example, the process of thermal vortex lattice melting can be mapped onto an insulator-to-superfluid transition of bosons. In this mapping, a vortex line is viewed as a world line of a boson with the z-axis mapped onto a “time”-axis and the vortex liquid, which is also entangled, represents the delocalized/superfluid state of the dual bosons [3]. The central result of the present work is that we find evidence in large-scale Monte Carlo (MC) computations that in a two-component Bose–Einstein condensate (BEC), the vortex lines support a state possessing properties of a vortex liquid simultaneously with properties of vortex lattice i.e. breakdown of translational symmetry.

Recent progress in creating and observing various mixtures of multi-component BEC has produced much interest in these systems. When BEC components are not spatially separated, the generic type of interaction between them is the current-current interaction (Andreev–Bashkin effect)[4] describing non-dissipative drag between the two superfluid components. Such a system in units where $\hbar = 1$ is described by the free energy density [4, 5, 6]

$$F = \frac{1}{2}\Bigg\{ m_1 n_1 \left(\frac{\nabla\theta_1}{m_1} - \mathbf{\Theta}\right)^2 + m_2 n_2 \left(\frac{\nabla\theta_2}{m_2} - \mathbf{\Theta}\right)^2 - \sqrt{m_1 m_2} n_d \left(\frac{\nabla\theta_1}{m_1} - \frac{\nabla\theta_2}{m_2}\right)^2 \Bigg\}, \qquad (1)$$

where m_1, m_2, θ_1 and θ_2 are the masses and the phases of the condensates while n_1, n_2 control the phase stiffnesses of the two components. Further, the drag coeficient n_d controls the density of one component dragged by the superfluid velocity of the other component. Since here we are interested in the physics of rotating system we include the field $\mathbf{\Theta}$ which accounts for rotation with angular velocity $\mathbf{\Omega} = \nabla \times \mathbf{\Theta} = 2\pi f \hat{\mathbf{z}}$, where $m_i f$ is the number of rotation-induced vortices per unit area of component i. We will use $f = 1/64$ throughout. In the following, we denote vortices with $2\pi l_{(i,j)}$ windings in $\theta_{(1,2)}$ with a pair of integers $(\Delta\theta_1 = 2\pi l_1, \Delta\theta_2 = 2\pi l_2) = (l_1, l_2)$. The last term in (1) is the current-current interaction[4] which may be caused by different reasons, such as intercomponent van der Waals interaction[4] or originating with the underlying optical lattice [5]. It was first considered in the contexts of the physics of ^{3}He -^{4}He mixtures and coexisting neutronic and protonic condensates in neutron stars. Various aspects of the rotational response of this system has been studied so far only for *positive* values of drag in context of $^3He - {}^4He$ mixtures [4] and BEC mixtures [7]. However, it has been recently shown that in optical lattices there arises an intriguing possibility to produce a BEC mixture with a *negative* inter-species drag n_d [5].

In this paper we address the physics of a rotating system with a negative intercomponent drag and find it being very rich. This is manifested in the situations where the usual notions from disordered versus ordered vortex states do not directly apply. Let us first briefly recapitulate the phase diagram of this system in the absence of rotation. Its main feature is that for significantly large drag $|n_d| > n_c$, the easiest topological defects to excite thermally are $(1, 1)$ vortex loops. Proliferation of these composite defects leads to a state with order only in the phase difference, a so-called super-counter-fluid [5, 6, 8]. In order to estimate the phase stiffness which is left in the system after the (1,1) vortex loops proliferate, one has to extract from the Eq. (1) the term which depends only on the gradients of the phase difference, which stiffness is thus unaffected by the proliferation of (1,1) loops. The corresponding separation of variables in the presence of rotation is given by

$$F = \frac{1}{2}\Bigg\{ \frac{\frac{n_1 n_2}{m_1 m_2} - \frac{n_d}{\sqrt{m_1 m_2}}\left(\frac{n_1}{m_2} + \frac{n_2}{m_1}\right)}{\frac{n_1}{m_1} + \frac{n_2}{m_2} - \frac{\sqrt{m_1 m_2}}{\tilde{\mu}^2} n_d} \times \left(\nabla\theta_1 - \nabla\theta_2 - (m_1 - m_2)\,\boldsymbol{\Theta}\right)^2 + \frac{1}{\frac{n_1}{m_1} + \frac{n_2}{m_2} - \frac{\sqrt{m_1 m_2}}{\tilde{\mu}^2} n_d} \times \left[\left(\frac{n_1}{m_1} - \sqrt{\frac{m_2}{m_1}}\frac{n_d}{\tilde{\mu}}\right)(\nabla\theta_1 - m_1\boldsymbol{\Theta}) + \left(\frac{n_2}{m_2} + \sqrt{\frac{m_1}{m_2}}\frac{n_d}{\tilde{\mu}}\right)(\nabla\theta_2 - m_2\boldsymbol{\Theta})\right]^2 \Bigg\}, \quad (2)$$

where $\tilde{\mu}^{-1} = m_1^{-1} - m_2^{-1}$.

After proliferation of (1,1) vortices it is the first term in (2) which accounts for the only phase stiffness remaining in the system, and we can renormalize the coefficient of the second term to zero and discard it. The complexity of the situation arising under rotation is that along with the (1,1) vortex loops excitations there are rotation-induced vortex lines. Vortex loops and lines affect each other's orderings and proliferation. Thus, we may ask (i) what are the ordering patterns of rotation-induced vortex lines in the model (1), (ii) how do rotation-induced vortex lines contribute to renormalization of stiffness and thus to symmetry breakdown patterns, and (iii) can ordering of the rotation-induced vortices signal the presence of a negative drag effect.

To address these questions, we have performed large-scale MC computations using discretization of Eq. (1) under rotation, in the Villain approximation [6]. Throughout, we use a temperature scale such that the temperature T at which two decoupled superfluids with equal masses and phase stiffnesses transition to normal fluids is $T = 3.3$. A negative intercomponent drag will tend to increase the temperature at which this transition occurs.

Consider first the simplest limit when $m_1 = m_2 = 1$ and $n_1 = n_2 = n$. Eq. (2) then simplifies to

$$F = \left(\frac{n}{4} - \frac{n_d}{2}\right)(\nabla(\theta_1 - \theta_2))^2 + \frac{n}{4}\left(\nabla(\theta_1 + \theta_2) - 2\boldsymbol{\Theta}\right)^2. \quad (3)$$

When $n_d = 0$, the condensates are decoupled and a rotating system forms two hexagonal lattices of the types (1,0) and (0,1). For $n_d < 0$, an attractive interaction between rotation-induced vortices results. Thus, in the ground state the system forms a triangular lattice of (1,1) vortices. Such a configuration minimizes the gradients in the first term in Eq. (3). In the simplest limit $m_1 = m_2 = 1$ and $n_1 = n_2 = n$ we have found regimes where the vortex lattice melts while vortices nonetheless retain their composite character. The system retains a symmetry in the phase difference thereby representing a "rotation-induced" super-counter-fluid state. Introducing a mass and density disparity $m_1 \neq m_2$ and $n_1 \neq n_2$ gives an entirely different ordering and symmetry breakdown. This is the main focus of this paper.

We study the spatial symmetry breakdown pattern and the effect of thermal fluctuations, by computing real space averages of vortex densities. They are produced by integrating the z-directed vortex segments along the z-axis, $\tilde{\nu}_i(\boldsymbol{r}_\perp) = L_z^{-1}\sum_z \nu_i^z(\boldsymbol{r}_\perp, z)$, with a subsequent averaging over typically 10^4 different configurations at a given temperature. $\nu_i^z(\boldsymbol{r}_\perp, z)$ is the vorticity of component i in the z-direction at $\boldsymbol{r} = (x, y, z)$ and $\boldsymbol{r}_\perp = (x, y)$ is the position in the xy-plane. Thus, for an elementary vortex on the numerical grid directed along z-axis, the quantity $\nu_i^z(\boldsymbol{r}_\perp, z)$ is nonzero and positive in lattice plaquette which corresponds to the center of the vortex. It is nonzero and negative for an antivortex, whence $\tilde{\nu}_i(\boldsymbol{r}_\perp)$ gives the average xy-position density of the rotation-induced vortices.

Let us consider the case $n_2/n_1 = 4$, $n_d/n_1 = -5.0$ and $m_2/m_1 = 2$. Now, since the vortex density is proportional to Ωm_i [9], there are twice as many vortices in component 2 as in component 1 for these parameters. The system exhibits a striking vortex ordering. Component 1 forms a triangular lattice, while component 2 with twice as many vortices, forms a honeycomb lattice. Every second vortex in the honeycomb lattice is co-centered with a vortex of the other component. This can be also viewed as an ordered equal mixture of (1,1) and (0,1) vortices. We find that the structure with a honeycomb plus hexagonal vortex lattice persists for a significant range of temperatures. Fig. 1a shows a real-space average and a $3d$ snapshot of a typical configuration of this spatial symmetry breakdown pattern at $T = 6.9$. This ordering has broken down at $T = 9.5$, where we observe a partial meltdown manifested in the disappearance of every second vortex position peak in the real-space averages. However, every other vorticity peak corresponding to a hexagonal sublattice co-centered with vortex lattice of component 1 survives. The reduction of the number of vorticity peaks in component 2, the corresponding change in the structure factor, along with a $3d$ snapshot of a typical vortex configuration, is shown on Fig. 1b. The structure factor of component i is defined as $S^{(i)}(\boldsymbol{k}_\perp) = \left|1/(L_x L_y f)\sum_{\boldsymbol{r}_\perp}\tilde{\nu}_i(\boldsymbol{r}_\perp)\mathrm{e}^{-\mathrm{i}\boldsymbol{r}_\perp\cdot\boldsymbol{k}_\perp}\right|^2$.

Let us finally turn to the case where $m_2/m_1 = 2$, but $n_2/n_1 = 16$. Now, with $n_d/n_1 = -2.5$, we find that at low temperatures, the system instead forms two square lattices. In the ground state the square lattice in component 2, which has twice as many vortices as component 1, is rotated 45 degrees with respect to the lattice of component 1, so that every second vortex is co-centered with a vortex of component 1 lattice, see Fig. 2a. Again this can be viewed as an equal mixture of (1,1) and (0,1) vortices. Note that, in contrast to the case of two-component vortex matter with only repulsive interactions [7, 10], here the vortex lattices are not interlaced. Here, the

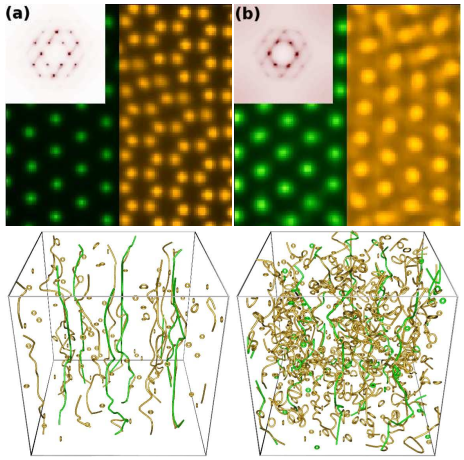

FIG. 1: (color online) Vortex orderings for the parameters $n_2/n_1 = 4$, $n_d/n_1 = -5.0$ and $m_2/m_1 = 2$. Panel (a) shows the low temperature phase, ($T = 6.90$), where vorticity averages (shown in gold for component 2 and green for component 1) produce a hexagonal vortex lattice in one component and a honeycomb lattice in the other component. Panel (b) shows the situation occurring at a higher temperature ($T = 9.52$), where a hexagonal sublattice of the honeycomb lattice melts, the number of vorticity peaks in real-space averages diminishes by a factor two, and the remaining hexagonal lattice is co-centered with a vortex lattice of component 1. The the insets in the top panels in part (a) and (b) show the structure factor evolution. The lower panels show a typical $3d$ vortex configuration in a $24 \times 24 \times 24$ segment of the system.

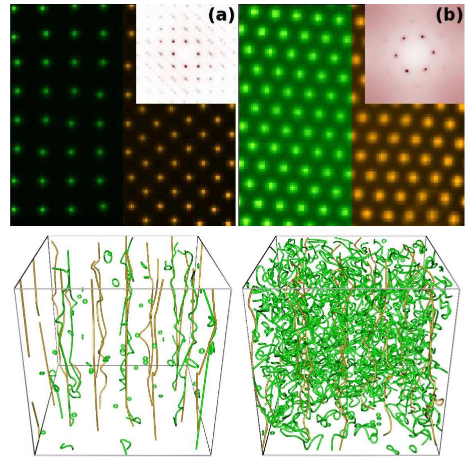

FIG. 2: (color online) Vortex orderings for the parameters $n_2/n_1 = 16$, $n_d/n_1 = -2.5$ and $m_2/m_1 = 2$. The $\boldsymbol{k}$-space inset is the full $\boldsymbol{k}$-space structure factor for component 1, in both panel (a) and (b). The left hand side in panel (a) and (b) is a realspace average of component 2 (yellow), while the right hand side is component 1 (green). Column (a) corresponds to the ordering in low-temperature ($T = 11.0$). Coulumn (b) shows the situation taking place at higher temperature ($T = 13.3$) where the green vortices (component 1) are in the phase corresponding to a dual superfluid bosonic density wave. It is far from obvious from the $3d$ picture in the panel (b) that component 1 breaks translational symmetry. However, when averaged over many configurations, we see that component 1 indeed breaks translational symmetry.

appearance of square symmetry is caused by attractive interactions between vortices of different types.

As the temperature is increased from $T = 11.0$ to $T = 13.3$, cf. Fig. 2, the evolution of the system is particularly remarkable: we observe a discontinuous phase transition, where in the real-space averages the number of vortex position peaks in component 1 *doubles*. This should be compared with the previous case of lower disparity of stiffnesses. There, in contrast, the system undergoes a transition to a state where vortex position peaks of the other component was reduced by a factor of two. Furthermore, both lattices change symmetry by collapsing onto a hexagonal co-centered configuration, as seen in the right panel of Fig. 2. A $3d$ snapshot of a part of the system, shown in the lower panel in Fig. 2, reveals that the process is accompanied by a rapid increase of vortex loops in component 1. Furthermore, the figure 3 shows the central feature of this state. Namely, the helicity modulus, equivalently the superfluid density computed according to the procedures in Ref. [6], for component 1 disappears essentially simultaneously with the structure factor for the square lattice in component 1. However, at the same time there emerges a nonzero triangular structure factor in component 1. It extends for a significant range of temperature *where the helicity modulus of component* 1 *is zero*. Therefore, the above observations are not related to a standard vortex-loop proliferation transition in the $3dXY$ universality class. If this behavior were associated with a standard vortex-loop proliferation transition of the vortices in component 1, the superfluid stiffness (helicity modulus) of this component would vanish simultaneously with the structure factor of the corresponding vortex lattice.

Thus, we have a quite remarkable situation. On the one hand, zero helicity modulus in z-direction indicates that vortices are entangled with each other like in a vortex liquid, a state which has a dual counterpart in superfluid bosons [3]. On the other hand, the vortex system nonetheless features a structure function which is characteristic of a vortex lattice, namely it has distinct peaks at reciprocal lattice vectors. Thus, the dual counterpart of the vortex system we found, is a bosonic superfluid density wave.

In terms of vortex matter this corresponds to the following situation. Vortices in component 1 in this state are largely co-centered with the vortex lattice of component 2, but at these temperatures constantly and freely switch from being co-centered with one to being co-centered with the another vortex at different points along the z-axis. In order for the number of vortex position peaks of component 1 to be double the number that is generated by the rotation, a large number of (1,0) vortex loops must be induced. Then the part of each (1,0) loop that is parallel to the (0,1) vortices have a tendency to be co-centered with a (0,1) vortex, breaking translational symmetry for this segment, while the remaining part of the (1,0) loop which is not parallel to the (0,1) vortices has a random position and does not break translational symmetry. Only at further elevated temperatures, a crossover takes place where vortex loops proliferate, and the vortices loose line tension and the structure factor vanishes, see Fig. 3.

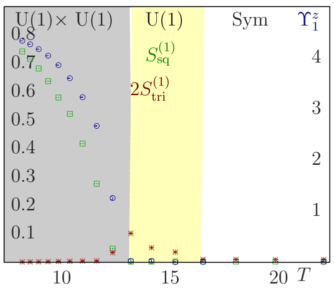

FIG. 3: (color online) Plot of the evolution of the structure factor for component 1 (red and green) when with increasing temperature the system undergoes a sequence of the phase transitions from the state with $U(1) \times U(1)$ broken symmetry to the state with $U(1)$ broken symmetry and finally to the fully symmetric state (denoted as "Sym"). The (green) squares represent the structure function of the *square lattice* in component 1, $S^{(1)}_{sq}$, at the Bragg-peaks at $\boldsymbol{k}_\perp = (0.7854, 0.00) \approx (\pi/4, 0)$. The (red) crosses represent the structure function of the *triangular lattice* in component 1, $S^{(1)}_{tri}$, at the Bragg-peak at $\boldsymbol{k}_\perp = (1.1781, 0.0982) \approx (3\pi/8, \pi/64)$. Furthermore, the (blue) circles represent the helicity modulus in the z-direction for component 1. It vanishes at the same temperature as the square lattice ordering ceases. However at the same temperature there appears a nonzero structure factor for a triangular lattice $S^{(1)}_{tri}$. This is accociated with the vortex state dual to bosonic superfluid density wave. The parameters are $n_2/n_1 = 16$, $n_d/n_1 = -2.5$ and $m_2/m_1 = 2$. The system size is $L \times L \times L$, with $L = 64$. Periodic boundary conditions are used in all directions, 10^5 sweeps are used for thermalization and 10^6 sweeps for collecting average values with sampling every $100^{\rm th}$ sweep.

In conclusion, we have considered two-component superfluids with a negative dissipationless drag. In the model Eq. (1), the underlying optical lattice plays only a microscopic role by providing a negative intercomponent drag through the mechanisms discussed in [5]. Thus , Eq. (1) describes the system at temperatures T larger than the vortex pinning energy of optical lattice E_p and thus there is no lattice pinning effect [11]. The vortex ordering pattern in this system is strongly affected by the negative dissipationless drag, resulting in the formation of square and honeycomb lattices. Observation of these different ordering symmetries in experiments would be the hallmark of intercomponent drag. At finite temperature there are phase transitions between states with different lattice symmetries. The main conclusion of our paper is that, apart from different patterns of spacial symmetry breakdown, the standard notions of vortex ordering single-component vortex matter do not directly apply in the case of two-component vortex matter with a negative drag. Namely, we have identified a state of vortex matter which is dual to a bosonic superfluid density wave, where one of the components breaks translational symmetry even though there is *no* symmetry broken in the order parameter space. In this regime, a standard experimental technique of a density snapshot with a significant averaging along the z-axis would indicate a vortex lattice even though this is not a superfluid state. Since this state is phase-disordered, it can be discriminated from superfluid vortex lattice via interference experiments. In an experimental situation, these effects will be naturally affected by density inhomogeneities present in traps. However, studies [12] of the effect of the presence of a trap on three dimensional vortex matter, suggest that the above states can be realizable in an extended area near the center of the trap.

This work was supported by the Norwegian Research Council Grants No. 158518/431 and No. 158547/431 (NANOMAT), and Grant No. 167498/V30 (STORFORSK).

[1] D. S Fisher, M. P. A. Fisher, and D. A. Huse, Phys. Rev. B **43**, 130 (1991).

[2] E. Babaev, A. Sudbø, and N. W. Ashcroft, Nature, **431**, 666 (2004); E. Smørgrav, J. Smiseth, E. Babaev, and A. Sudbø, Phys. Rev. Lett. **94**, 096401 (2005); *ibid* **95**, 135301 (2005); E.Babaev and N.W. Ashcroft, Nature Physics **3**, 530 (2007).

[3] D. R. Nelson, Phys. Rev. Lett. **60**, 1973 (1988); M. P. A. Fisher and D. H. Lee, Phys. Rev. B **39**, 2756 (1989).

[4] A. F. Andreev and E. Bashkin, Sov. Phys. JETP **42**, 164 (1975); D. V. Fil, S. I. Shevchenko, Phys. Rev. A **72**, 013616 (2005).

[5] A. B. Kuklov and B. V. Svistunov, Phys. Rev. Lett. **90**, 100401 (2003); V. Kaurov, A. Kuklov, and A. Meyerovich, Phys. Rev. Lett. **95**, 090403 (2005).

[6] E. K. Dahl, E. Babaev, S. Kragset, and A. Sudbø, Phys. Rev. B **77,** 144519 (2008).

[7] E. K. Dahl, E. Babaev, and A. Sudbø, Phys. Rev. B **78**, 144510 (2008).

[8] A. Kuklov, *et.al.* Phys. Rev. Lett. **92**, 030403 (2004); Ann. of Phys. **321**, 1602 (2006).

[9] R. Feynman *Statistical Mechanics*, Addison Wesley (1990).

[10] E. J. Mueller and T.-L. Ho, Phys. Rev. Lett. **88**, 180403 (2002).

[11] S. Tung, V. Schweikhard, and E. A. Cornell, Phys. Rev. Lett. **97**, 240402 (2006)

[12] S. Kragset, E. Babaev, and A. Sudbø, Phys. Rev. Lett. **97**, 170403 (2006); Phys. Rev. A **77**, 043605 (2008).